Anal. Chem. **2006,** *78,* 2352−2359

Control of the Oxygen Dependence of an Implantable Polymer/Enzyme Composite Biosensor for Glutamate

Colm P. McMahon,[†] Gaia Rocchitta,[†,‡] Pier A. Serra,[†,‡] Sarah M. Kirwan,[†] John P. Lowry,[‡] and Robert D. O'Neill*[,†]

UCD School of Chemistry and Chemical Biology, University College Dublin, Belfield, Dublin 4, Ireland, and UCD School of Biomolecular and Biomedical Sciences, University College Dublin, Belfield, Dublin 4, Ireland

Biosensors for glutamate (Glu) were fabricated from Teflon-coated Pt wire (cylinders and disks), modified with the enzyme glutamate oxidase (GluOx) and electrosynthesized polymer PPD, poly(*o*-phenylenediamine). The polymer/enzyme layer was deposited in two configurations: enzyme before polymer (GluOx/PPD) and enzyme after polymer (PPD/GluOx). These four biosensor designs were characterized in terms of response time, limit of detection, Michaelis−Menten parameters for Glu (J_{max} and K_M(Glu)), sensitivity to Glu in the linear response region, and dependence on oxygen concentration, $K_M(O_2)$. Analysis showed that the two polymer/enzyme configurations behaved similarly on both cylinders and disks. Although the two geometries showed different behaviors, these differences could be explained in terms of higher enzyme loading density on the disks; in many analyses, the four designs behaved like a single population with a range of GluOx loading. Enzyme loading was the key to controlling the $K_M(O_2)$ values of these first generation biosensors. The counterintuitive, and beneficial, behavior that biosensors with higher GluOx loading displayed a lower oxygen dependence was explained in terms of the effects of enzyme loading on the affinity of GluOx for its anionic substrate. Some differences between the properties of surface immobilized GluOx and glucose oxidase are highlighted.

L-Glutamate (Glu) is the most widespread excitatory neurotransmitter in the mammalian central nervous system,[1] plays a major role in a broad range of brain functions, and has been implicated in a number of neurological disorders.[2] Indeed, the development of devices for Glu detection has become an important research area due to the value of monitoring this key amino acid in a number of complex matrixes, including food processing,[3,4] cell cultures,[5−7] tissue slices ex vivo,[8,9] and intact brain in vivo.[10−15]

A number of designs of biosensors for Glu monitoring have been reported and, although Glu receptors[16] and Glu dehydrogenase[8,17,18] have been used as sensing elements, these devices are more commonly based on the stereospecific oxidative deamination of Glu, catalyzed by Glu oxidase (GluOx: MW_r, 140 kDa; solution K_M, 0.21 mM in neutral phosphate buffer; pI, 6.2;[19] see reactions 1 and 2.[19,20])

$$\text{L-glutamate} + H_2O + \text{GluOx/FAD} \rightarrow \alpha\text{-ketoglutarate} + NH_3 + \text{GluOx/FADH}_2 \quad (1)$$

$$\text{GluOx/FADH}_2 + O_2 \rightarrow \text{GluOx/FAD} + H_2O_2 \quad (2)$$

$$H_2O_2 \rightarrow O_2 + 2H^+ + 2e \quad (3)$$

Signal transduction systems employed in Glu biosensors include optical technologies,[21−23] but usually electrochemical

* To whom correspondence should be addressed. Phone: +353-1-7162314. Fax: +353-1-7162127. E-mail: Robert.ONeill@UCD.ie.

† UCD School of Chemistry and Chemical Biology.

‡ UCD School of Biomolecular and Biomedical Sciences.

(1) Orrego, F.; Villanueva, S. *Neuroscience* **1993**, *56*, 539−555.
(2) Belsham, B. *Hum. Pharmacol. Clin. Exp.* **2001**, *16*, 139−146.
(3) Moser, I.; Jobst, G.; Urban, G. A. *Biosens. Bioelectron.* **2002**, *17*, 297−302.
(4) Nakorn, P. N.; Suphantharika, M.; Udomsopagit, S.; Surareungchai, W. *World J. Microbiol. Biotechnol.* **2003**, *19*, 479−485.
(5) Kurita, R.; Hayashi, K.; Torimitsu, K.; Niwa, O. *Anal. Sci.* **2003**, *19*, 1581−1585.
(6) O'Neill, R. D.; Chang, S. C.; Lowry, J. P.; McNeil, C. J. *Biosens. Bioelectron.* **2004**, *19*, 1521−1528.
(7) Mikeladze, E.; Schulte, A.; Mosbach, M.; Blochl, A.; Csoregi, E.; Solomonia, R.; Schumann, W. *Electroanalysis* **2002**, *14*, 393−399.
(8) Qhobosheane, M.; Wu, D. H.; Gu, G. R.; Tan, W. H. *J. Neurosci. Methods* **2004**, *135*, 71−78.
(9) Isobe, Y.; Nishihara, K. *Brain Res. Bull.* **2002**, *58*, 401−404.
(10) Burmeister, J. J.; Gerhardt, G. A. *Trends Anal. Chem.* **2003**, *22*, 498−502.
(11) Matsushita, Y.; Shima, K.; Nawashiro, H.; Wada, K. *J. Neurotrauma* **2000**, *17*, 143−153.
(12) Hu, Y.; Mitchell, K. M.; Albahadily, F. N.; Michaelis, E. K.; Wilson, G. S. *Brain Res.* **1994**, *659*, 117−125.
(13) Burmeister, J. J.; Pomerleau, F.; Palmer, M.; Day, B. K.; Huettl, P.; Gerhardt, G. A. *J. Neurosci. Methods* **2002**, *119*, 163−171.
(14) Cui, J.; Kulagina, N. V.; Michael, A. C. *J. Neurosci. Methods* **2001**, *104*, 183−189.
(15) Kulagina, N. V.; Shankar, L.; Michael, A. C. *Anal. Chem.* **1999**, *71*, 5093−5100.
(16) Minami, H.; Sugawara, M.; Odashima, K.; Umezawa, Y.; Uto, M.; Michaelis, E. K.; Kuwana, T. *Anal. Chem.* **1991**, *63*, 2787−2795.
(17) Montagne, M.; Durliat, H.; Comtat, M. *Anal. Chim. Acta* **1993**, *278*, 25−33.
(18) Cosford, R. J. O.; Kuhr, W. G. *Anal. Chem.* **1996**, *68*, 2164−2169.
(19) Kusakabe, H.; Midorikawa, Y.; Fujishima, T.; Kuninaka, A.; Yoshino, H. *Agric. Biol. Chem.* **1983**, *47*, 1323−1328.
(20) Mikeladze, E.; Collins, A.; Sukhacheva, M.; Netrusov, A.; Csoregi, E. *Electroanalysis* **2002**, *14*, 1052−1059.
(21) Dremel, B. A. A.; Schmid, R. D.; Wolfbeis, O. S. *Anal. Chim. Acta* **1991**, *248*, 351−359.
(22) Wang, A. J.; Arnold, M. A. *Anal. Chem.* **1992**, *64*, 1051−1055.

10.1021/ac0518194 CCC: $33.50
Published on Web 03/07/2006

oxidation of enzymatically produced H_2O_2 (reactions 2 and 3) is exploited. A variety of chemistries have been explored for efficient detection of H_2O_2 generated by GluOx, including direct oxidation on metals[12,24−29] (usually coated with a permselective polymer to block interference), metallicized carbon[30,31] or conducting polymer-coated Pt,[32] and catalytic oxidation using horseradish peroxidase coupled to a redox polymer.[6,15,20,33,34]

Biosensors in general, and especially those designed for tissue implantation,[35−39] must fulfill the following minimum criteria for reliable monitoring of the target analyte: appropriate size and biocompatibility properties, good sensitivity to the enzyme substrate, effective rejection of electroactive interference, and low sensitivity to changes in pO_2 over the range of substrate and oxygen concentrations relevant to the intended application. We recently reported preliminary data and analysis of the oxygen dependence of implantable Glu biosensors incorporating GluOx in a poly(*o*-phenylenediamine), PPD, interference-rejecting layer electrosynthesized onto 125-μm-diameter Pt cylinders (Pt_C) and disks (Pt_D).[40] This represented the first quantitative study of the oxygen dependence of GluOx at low micromolar levels of oxygen and demonstrated that GluOx immobilized on Pt functioned efficiently, even at low pO_2.[12] Surprisingly, however, the disk-based design, which displayed the higher Glu sensitivity in the linear response calibration region, had a lower (better) oxygen dependence than the corresponding cylinder devices.[40] Here, we extend the experimental data and analysis significantly by determining the Michaelis−Menten kinetic parameters and the oxygen dependence of four Pt/GluOx-PPD designs to investigate this unexpected behavior.

Different Pt/GluOx-PPD configurations were explored to manipulate biosensor Glu sensitivity for two main reasons: first, as part of our ongoing efforts to increase substrate sensitivity sufficiently to detect the normally low micromolar levels of Glu in brain extracellular fluid (ECF); second, and more importantly for the present study, to influence the oxygen demand of the system (reaction 2). Substrate sensitivity of Pt/oxidase-PPD biosensors can be affected by the Pt geometry[40] and by the order of enzyme/polymer deposition on the Pt surface.[41] We therefore used biosensors fabricated from Pt disks and cylinders and GluOx immobilization before and after electrosynthesis of the PPD to determine the oxygen profile of devices with different Glu sensitivities. These studies reveal that surface GluOx loading can be used to control biosensor oxygen dependence in a counterintuitive direction: higher loading led to lower sensitivity to oxygen in the linear range of Glu response. The details of this effect are very different from those for surface immobilized glucose oxidase (GOx),[41,42] setting limits on the usefulness of GOx as a model enzyme in biosensor design.

EXPERIMENTAL SECTION

Instrumentation and Software. Experiments were computer-controlled, with data collection accomplished using either a Biodata Microlink interface, a PowerLab 8/30 (ADInstruments Inc., U.K.), or a National Instruments (NI, Austin, TX) AT-MIO-16 data acquisition board linked to a low-noise, low-damping potentiostat (Biostat II, Electrochemical and Medical Systems, Newbury, U.K.). In-house software was written in QuickBASIC (version 4.0) and NI LabWindows (version 2.1) QuickBASIC environments to perform amperometric experiments and to collect, plot, and do a preliminary analysis of the data.

Response times were recorded in constantly stirred solution, using the PowerLab module operating at a data acquisition rate of 100 Hz. A $t_{90\%}$ parameter was defined as the time taken for the analyte response to reach 90% of its maximum value from the start of the current upswing and is similar to definitions used previously.[15,24,43] The raw data was filtered digitally, using a weighted moving average, to remove small noise spikes.[44] Although effective at reducing noise, this procedure had only a minor effect on the response time itself. For example, the fastest $t_{90\%}$ response observed (H_2O_2 on bare Pt) was increased by only 0.1 s by this form of digital filtering. The limit of detection (LOD) was determined using the widely used criterion of three times the SD of the baseline.[29,45]

Biosensor Fabrication and Calibration. Pt cylinders (Pt_C, 125-μm diameter, 1 mm long) were fabricated from Teflon-coated Pt wire (Advent Research Materials, Suffolk, U.K.). GluOx (EC 1.4.3.11, 200 U mL^{-1}, Yamasa Corp., Japan) was deposited onto the metal surface by dip-evaporation (1−5 dips)[28] and immobilized by amperometric electropolymerization (+700 mV vs SCE) in 300 mM *o*-phenylenediamine containing 5 mg mL^{-1} bovine serum albumin in phosphate buffered saline (PBS, pH 7.4),[46] as described previously to form Pt_C/GluOx/PPD biosensors.[28] Pt disks (Pt_D) were fabricated by cutting the Teflon-coated wire transversely to produce 125-μm diameter disks, and Pt_D/GluOx/PPD biosensors were fabricated as for Pt_C.

The alternative polymer/enzyme configuration (enzyme deposited by dip-evaporation after the polymerization step) was also

(23) Marquette, C. A.; Degiuli, A.; Blum, L. J. *Biosens. Bioelectron.* **2003**, *19*, 433−439.
(24) Berners, M. O. M.; Boutelle, M. G.; Fillenz, M. *Anal. Chem.* **1994**, *66*, 2017−2021.
(25) Cooper, J. M.; Foreman, P. L.; Glidle, A.; Ling, T. W.; Pritchard, D. J. *J. Electroanal. Chem.* **1995**, *388*, 143−149.
(26) Cosnier, S.; Innocent, C.; Allien, L.; Poitry, S.; Tsacopoulos, M. *Anal. Chem.* **1997**, *69*, 968−971.
(27) Poitry, S.; Poitry-Yamate, C.; Innocent, C.; Cosnier, S.; Tsacopoulos, M. *Electrochim. Acta* **1997**, *42*, 3217−3223.
(28) Ryan, M. R.; Lowry, J. P.; O'Neill, R. D. *Analyst* **1997**, *122*, 1419−1424.
(29) Burmeister, J. J.; Gerhardt, G. A. *Anal. Chem.* **2001**, *73*, 1037−1042.
(30) White, S. F.; Turner, A. P. F.; Bilitewski, U.; Schmid, R. D.; Bradley, J. *Anal. Chim. Acta* **1994**, *295*, 243−251.
(31) Chang, K. S.; Hsu, W. L.; Chen, H. Y.; Chang, C. K.; Chen, C. Y. *Anal. Chim. Acta* **2003**, *481*, 199−208.
(32) Rahman, M. A.; Kwon, N. H.; Won, M. S.; Choe, E. S.; Shim, Y. S. *Anal. Chem.* **2005**, *77*, 4854−4860.
(33) Shi, G. Y.; Yamamoto, K.; Zhou, T. S.; Xu, F.; Kato, T.; Jin, J. Y.; Jin, L. T. *Electrophoresis* **2003**, *24*, 3266−3272.
(34) Castillo, J.; Isik, S.; Blochl, A.; Pereira-Rodrigues, N.; Bedioui, F.; Csoregi, E.; Schuhmann, W.; Oni, J. *Biosens. Bioelectron.* **2005**, *20*, 1559−1565.
(35) Khan, A. S.; Michael, A. C. *Trends Anal. Chem.* **2003**, *22*, 503−508.
(36) Wilson, G. S.; Gifford, R. *Biosens. Bioelectron.* **2005**, *20*, 2388−2403.
(37) Wilson, G. S.; Hu, Y. B. *Chem. Rev.* **2000**, *100*, 2693−2704.
(38) O'Neill, R. D.; Lowry, J. P.; Mas, M. *Crit. Rev. Neurobiol.* **1998**, *12*, 69−127.
(39) Pantano, P.; Kuhr, W. G. *Electroanalysis* **1995**, *7*, 405−416.
(40) McMahon, C. P.; O'Neill, R. D. *Anal. Chem.* **2005**, *77*, 1196−1199.
(41) McMahon, C. P.; Killoran, S. J.; O'Neill, R. D. *J. Electroanal. Chem.* **2005**, *580*, 193−202.
(42) Zhang, Y. N.; Wilson, G. S. *Anal. Chim. Acta* **1993**, *281*, 513−520.
(43) Burmeister, J. J.; Palmer, M.; Gerhardt, G. A. *Anal. Chim. Acta* **2003**, *481*, 65−74.
(44) O'Neill, R. D.; Fillenz, M. *Neuroscience* **1985**, *14*, 753−763.
(45) Mocak, J.; Bond, A. M.; Mitchell, S.; Scollary, G. *Pure Appl. Chem.* **1997**, *69*, 297−328.
(46) Craig, J. D.; O'Neill, R. D. *Analyst* **2003**, *128*, 905−911.

investigated: Pt_C/PPD/GluOx and Pt_D/PPD/GluOx, for which the enzyme was immobilized by exposure to glutaraldehyde vapor.[41] After rinsing and a settling period at +700 mV in fresh PBS, amperometric calibrations were carried out to determine the apparent Michaelis−Menten parameters (J_{max} and K_M(Glu); see below) and the linear region sensitivity (0−100 μM) of the biosensors to Glu and H_2O_2 in quiescent air-saturated buffer, unless stated otherwise. All electropolymerizations and calibrations were performed in a standard three-electrode glass electrochemical cell containing 20 mL PBS at room temperature. A saturated calomel electrode (SCE) was used as the reference electrode, and a large stainless steel needle served as the auxiliary electrode.

Monitoring Dissolved Oxygen. A self-calibrating commercial membrane-covered amperometric oxygen sensor (~1 cm diameter) was used to quantify solution oxygen concentration as described previously.[47] The model used was a CellOx 325 connected to an Oxi 340A meter (Wissenschaftlich-Technische Werkstätten GmbH from Carl Stuart Ltd., Dublin, Ireland), incorporating a temperature probe for automatic compensation. Reliable quantification of O_2 using this device required constant stirring of the solution at a rate of ~3 Hz, a condition that also ensured homogeneity of the pO_2 throughout the cell. The CellOx 325 range was 0.0−199.9% O_2 (100% corresponding to air saturation) with a resolution of 0.1%. This percentage was converted to an estimated concentration of O_2 by taking 200 μM to correspond to 100%.[42,48]

To avoid contamination of the PBS by oxygen, the electrochemical cell was contained within an Atmosbag (Sigma),[47] a two-hand 0.003-in. gauge polyethylene bag that was sealed and filled with N_2 during experiments, inflating to a volume of 280 L. After adding an aliquot of Glu, air was allowed into the system slowly by opening the bag slightly. Oxygen sensor data and biosensor data were recorded simultaneously through the transition from N_2 saturation to ambient air concentration.

Kinetic Model and Data Analysis. A number of sophisticated mathematical models of the behavior of enzymes in membranes have been described.[49−53] These complex analyses are often needed to understand and optimize the behavior of thick or conducting layers;[53,54] however, a recent study has shown that substrate diffusion is not limiting for PPD layers incorporating enzyme,[55] due to their relatively small thickness.[53] This allows a basic Michaelis−Menten analysis to be used here, offering more readily accessible insights into factors affecting the responsiveness of biosensors fabricated from ultrathin (10−30 nm)[46,56−58] insulating polymers, such as PPD.

$$J_{Glu} = \frac{J_{max}}{1 + K_M(Glu)/[Glu]} \tag{4}$$

A two-substrate model is necessary to describe the kinetics of oxidase enzymes under conditions of varying concentration of both substrate and cosubstrate.[59,60] When the concentration of the cosubstrate is constant, however, the two-substrate equation simplifies to the one-substrate Michaelis−Menten form (eq 4), in which the current density for the biosensor Glu response, J_{Glu}, is a measure of the overall rate of the enzyme reaction, and J_{max} is the J_{Glu} value at enzyme saturation. Different values of J_{max} determined under the same conditions reflect differences in the amount of active enzyme on the surface,[41] provided the sensitivity of the electrode to H_2O_2 (reaction 3) does not vary, as is the case for the PPD-modified Pt cylinders and disks used here.[41,61,62]

$$E + S \underset{k_{-1}}{\overset{k_1}{\rightleftharpoons}} ES \xrightarrow{k_2} E + P \tag{5}$$

$$K_M = \frac{k_{-1} + k_2}{k_1} \tag{6}$$

The Michaelis constant, K_M, is defined in terms of the rate constants for the generalized reactions (reaction 5) describing the conversion of substrate (S) to product (P), catalyzed by enzyme (E) (see eq 6[63]). When eq 4 is used to approximate the two-substrate case, the K_M is more complex, containing cosubstrate terms. K_M is then the apparent Michaelis constant and phenomenologically defines the concentration of substrate that gives half the J_{max} response. Thus, changes in K_M are often sensitive to the binding constant, k_1, and have often been interpreted in terms of barriers to substrate/enzyme binding,[64,65] as well as changes in oxygen demand.[42]

$$J_{Glu} = \frac{J'_{max}}{1 + K_M(O_2)/[O_2]} \tag{7}$$

Alternatively, if the concentration of Glu is fixed and O_2 levels are changed, then eq 7 can be used to analyze the oxygen dependence of the Glu signal,[40,47] for which J'_{max} is the maximum (plateau) response for a particular concentration of Glu and $K_M(O_2)$ is the apparent Michaelis constant for oxygen. The option of using a single two-substrate equation, such as eq 32 in ref 59 or eq 1 in ref 66 that expresses explicitly the true Michaelis constants for both substrate and cosubstrate, was not used in this

(47) Dixon, B. M.; Lowry, J. P.; O'Neill, R. D. *J. Neurosci. Methods* **2002**, *119*, 135−142.
(48) Bourdillon, C.; Thomas, V.; Thomas, D. *Enzyme Microb. Technol.* **1982**, *4*, 175−180.
(49) Albery, W. J.; Bartlett, P. N. *J. Electroanal. Chem.* **1985**, *194*, 211−222.
(50) Bartlett, P. N.; Pratt, K. F. E. *Biosens. Bioelectron.* **1993**, *8*, 451−462.
(51) Phanthong, C.; Somasundrum, M. *J. Electroanal. Chem.* **2003**, *558*, 1−8.
(52) Baronas, R.; Ivanauskas, F.; Ivanauskas, F.; Kulys, J. *J. Math. Chem.* **2004**, *35*, 199−213.
(53) Gooding, J. J.; Hall, E. A. H.; Hibbert, D. B. *Electroanalysis* **1998**, *10*, 1130−1136.
(54) Baronas, R.; Ivanauskas, F.; Kulys, J. *Sensors* **2003**, *3*, 248−262.
(55) De Corcuera, J. I. R.; Cavalieri, R. P.; Powers, J. R. *J. Electroanal. Chem.* **2005**, *575*, 229−241.
(56) Malitesta, C.; Palmisano, F.; Torsi, L.; Zambonin, P. G. *Anal. Chem.* **1990**, *62*, 2735−2740.
(57) Sohn, T. W.; Stoecker, P. W.; Carp, W.; Yacynych, A. M. *Electroanalysis* **1991**, *3*, 763−766.
(58) Myler, S.; Eaton, S.; Higson, S. P. J. *Anal. Chim. Acta* **1997**, *357*, 55−61.
(59) Leypoldt, J. K.; Gough, D. A. *Anal. Chem.* **1984**, *56*, 2896−2904.
(60) Gooding, J. J.; Hall, E. A. H. *Electroanalysis* **1996**, *8*, 407−413.
(61) Lowry, J. P.; O'Neill, R. D. *Electroanalysis* **1994**, *6*, 369−379.
(62) McMahon, C. P.; Killoran, S. J.; Kirwan, S. M.; O'Neill, R. D. *J. Chem. Soc. Chem. Commun.* **2004**, 2128−2130.
(63) Mell, L. D.; Maloy, J. T. *Anal. Chem.* **1975**, *47*, 299−307.
(64) Compagnone, D.; Federici, G.; Bannister, J. V. *Electroanalysis* **1996**, *7*, 1151−1155.
(65) Sasso, S. V.; Pierce, R. J.; Walla, R.; Yacynych, A. M. *Anal. Chem.* **1990**, *62*, 1111−1117.
(66) Ikeda, T.; Katasho, I.; Kamei, M.; Senda, M. *Agric. Biol. Chem.* **1984**, *48*, 1969−1976.

analysis because the apparent Michaelis constants, defined separately, are analytically more straightforward, are useful for defining the linear range for Glu responses (~0.5 K_M(Glu), eq 4), and influence the Glu slope in the linear region, that is, ~J_{max}/K_M(Glu) (see eqs 8 and 9). The smaller the value of $K_M(O_2)$ in eq 7, the lower the oxygen dependence because higher oxygen affinity leads to oxygen saturation at lower pO_2, thereby reducing biosensor dependency at higher pO_2 levels.

Nonlinear regression analysis of the Glu response (eq 4), expressed in current density, and the oxygen dependence of the Glu signal (eq 7) were carried out using a software package (Prism, GraphPad Software, Inc., San Diego, CA). Linear regression was performed on the Glu dependence of the biosensor signal (0−100 μM) to obtain an experimental value of the linear region slope (LRS). Values of J_{max}, K_M(Glu), LRS, and $K_M(O_2)$ are presented as mean ± SEM, with n = number of biosensors; response times are reported as mean ± SD, with n = number of electrodes × determinations. The statistical significance of differences observed between responses for the various designs was calculated using Student's two-tailed unpaired t-tests on the absolute current densities, slopes, or Michaelis−Menten parameters.

RESULTS AND DISCUSSION

Biosensor Designs. Four configurations based on Pt coated with GluOx and PPD are reported here. The classical design,[28] which was the first of these used for brain implantation,[67] involves a Pt wire cylinder (125-μm diameter, 1-mm length) onto which enzyme is deposited by dip evaporation, followed by electrosynthesis of the permselective polymer, Pt_C/GluOx/PPD. These devices show relatively low Glu sensitivity,[40] and in a recent study, we demonstrated that the corresponding enzyme/polymer configuration deposited on disks made from the same wire (Pt_D/GluOx/PPD) showed significantly higher Glu sensitivity in the linear response region, coupled with a lower dependence on solution pO_2.[40] A main aim of this work was to investigate this apparently contradictory behavior of higher substrate sensitivity combined with lower oxygen dependence.

Another recent report showed that, for glucose biosensors incorporating PPD and GOx, depositing the enzyme after the polymerization step enhanced the sensitivity of both disk- and cylinder-based devices.[42] We also investigate here, therefore, the Glu and oxygen responses of the corresponding polymer/enzyme arrangements for GluOx: Pt_C/PPD/GluOx and Pt_D/PPD/GluOx.

Response Time and Limit of Detection. A number of aspects of the structure and behavior of Pt/oxidase-PPD biosensors indicate that their response is determined by enzyme kinetics, and not by diffusion through the polymer/enzyme composite (PEC) layer. First, the thickness of these PPD-based insulating layers (10−30 nm),[46,56−58] serving as both permselective barrier and immobilization matrix, is of the order that has been shown theoretically not to be limited by diffusion within the enzyme-containing layer. [53,55] Second, the response time of oxidase/PPD-based biosensors is fast,[68] being determined by the mixing time in stirred solution.[24,56] This contrasts with oxidase-containing biosensors incorporating thicker films, such as redox hydrogels (~30 s)[7,15,69] and polypyrrole films (~1 min).[56,70]

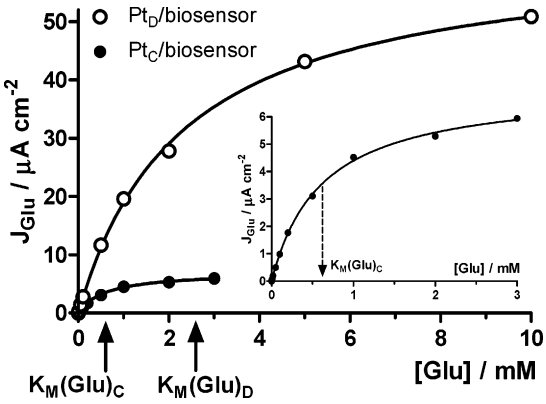

Figure 1. Sample experimental Glu calibration data, expressed as current density, and nonlinear regression analysis (eq 4) for both cylinder (Pt_C/GluOx/PPD, R^2 = 0.9992) and disk (Pt_D/GluOx/PPD, R^2 = 0.9995) biosensors, highlighting the different K_M(Glu) values (arrows) and J_{max} values of these two designs. Inset: Close-up of the Pt_C/GluOx/PPD plot. See Table 1 for mean calibration parameters of large populations of these two configurations.

Table 1. Mean Values ± SEM for the Two Apparent Michaelis-Menten Parameters (eq 4) and Experimentally Determined Linear Region Slope (LRS) for Each of the Four Biosensor Designs[a]

sensor design	J_{max} µA cm^{-2}	K_M(Glu) mM	LRS nA cm^{-2} µM^{-1}
Pt_C/GluOx/PPD (34)	9 ± 1	0.7 ± 0.1	13 ± 2
Pt_D/GluOx/PPD (46)	136 ± 15	4.8 ± 0.6	28 ± 2
Pt_C/PPD/GluOx (20)	8 ± 1	0.9 ± 0.1	8 ± 1
Pt_D/PPD/GluOx (16)	71 ± 7	2.3 ± 0.3	32 ± 4

[a] Number of biosensors in brackets.

To confirm that the response times of the biosensor designs described here were consistent with the kinetic model used, we determined $t_{90\%}$ for both H_2O_2 and Glu using addition of aliquots to continually stirred solutions. The Pt_D/GluOx/PPD design was chosen for this study because it showed the greatest enzyme loading density (see below) and, therefore, was most likely to deviate from ultrathin behavior.[53,55] The $t_{90\%}$ value for H_2O_2 at bare Pt_D was 1.2 ± 0.6 s (mean ± SD, n = 8 sensors × 5 determinations), and gives a measure of the mixing time in the electrochemical cell under the stirring conditions used. Following deposition of the GluOx/PPD layer, $t_{90\%}$ for H_2O_2 increased slightly but significantly to 1.8 ± 0.6 s (n = 40, p < 0.0001, as compared with the bare Pt_D metal). The value of $t_{90\%}$ for the Glu response at these Pt_D/GluOx/PPD biosensors was 3.0 ± 1.2 s (n = 40). Therefore, even for the design with the highest GluOx loading (Pt_D/GluOx/PPD; see Figure 1 and Table 1), the involvement of GluOx in the generation of the H_2O_2 signal (Glu mass transport and reaction kinetics: reactions 1 and 2) added only ~1 s to the response time, consistent with minimal hindrance of Glu access to the enzyme by the PPD layer. The corresponding response time for Glu at the Pt_C/GluOx/PPD cylinder design, which

(67) Lowry, J. P.; Ryan, M. R.; O'Neill, R. D. *Anal. Commun.* **1998**, *35*, 87−89.
(68) Lowry, J. P.; McAteer, K.; El Atrash, S. S.; Duff, A.; O'Neill, R. D. *Anal. Chem.* **1994**, *66*, 1754−1761.
(69) Castillo, J.; Blochl, A.; Dennison, S.; Schuhmann, W.; Csoregi, E. *Biosens. Bioelectron.* **2005**, *20*, 2116−2119.
(70) Yoshida, S.; Kanno, H.; Watanabe, T. *Anal. Sci.* **1995**, *11*, 251−256.

showed a 15-fold smaller mean J_{max} value (Table 1), was 2.4 ± 0.9 s (n = 12 sensors × 2 determinations), only marginally less than that for the disk design (p < 0.05). The $t_{90\%}$ values for these biosensors showed no significant dependence on concentration up to the maximum determined (100 μM for H_2O_2 and 2 mM for Glu).

There was no major difference between the LOD values (μM Glu, n = 8) for the four designs: Pt_C/GluOx/PPD (0.3 ± 0.1), Pt_D/GluOx/PPD (0.5 ± 0.1), Pt_C/PPD/GluOx (0.3 ± 0.1), and Pt_D/PPD/GluOx (0.4 ± 0.1), indicating comparable suitability for detection of low Glu levels in many biological applications, other factors being equal.

Michaelis−Menten Model. The concentration of Glu in many biological applications is low. For example, values reported under physiological conditions are normally below 10 μM for cerebrospinal fluid[71,72] and brain ECF,[73−75] although 100 μM levels have been detected in the ECF following brain trauma.[76] Thus, a critical property of GluOx-based biosensors is high sensitivity in the linear region, whereas with a solution K_M(Glu) value of 0.2 mM,[19] the range of linearity (up to 0.5 K_M(Glu)) is not a major issue.

$$\underset{[Glu]\to 0}{\mathrm{Lt}} J_{Glu} = \frac{J_{max}}{1 + K_M/[Glu]} = \frac{J_{max}[Glu]}{[Glu] + K_M} \approx \frac{J_{max}}{K_M}[Glu] \quad (8)$$

$$\frac{J_{max}}{K_M} \approx \mathrm{LRS} \quad (9)$$

The limiting form of the Michaelis−Menten equation (eq 4), as the concentration of Glu approaches zero, defines a relationship between J_{max}, K_M(Glu) and the linear region slope (LRS; eqs 8 and 9), giving LRS ≈ J_{max}/K_M(Glu). Clearly, a good LRS requires a high loading of active enzyme (J_{max}) while maintaining K_M(Glu) as low as possible. The values of J_{max} and K_M(Glu) were determined from full calibrations for the Pt_C/GluOx/PPD and Pt_D/GluOx/PPD designs reported recently[40] to investigate the factors endowing Pt_D/GluOx/PPD devices with significantly greater LRS as compared to Pt_C/GluOx/PPD biosensors.

Examples of individual full calibration plots for Pt_C/GluOx/PPD and Pt_D/GluOx/PPD configurations are shown in Figure 1. The fit (R^2 value) to eq 4 was excellent in both cases, 0.9992 (Pt_C) and 0.9995 (Pt_D), indicating the appropriateness of the Michaelis−Menten model. Equation 9 was tested by determining the two Michaelis−Menten parameters for each biosensor, calculating their ratio (J_{max}/K_M), and plotting this ratio against the experimentally measured LRS for the corresponding electrode. The linear regression slope of 1.1 ± 0.1 (R^2 = 0.97, n = 54; see Figure 2) agrees well with the predicted value of unity (eq 9) and illustrates the suitability of the single substrate Michaelis−Menten analysis for both cylinder and disk biosensors.

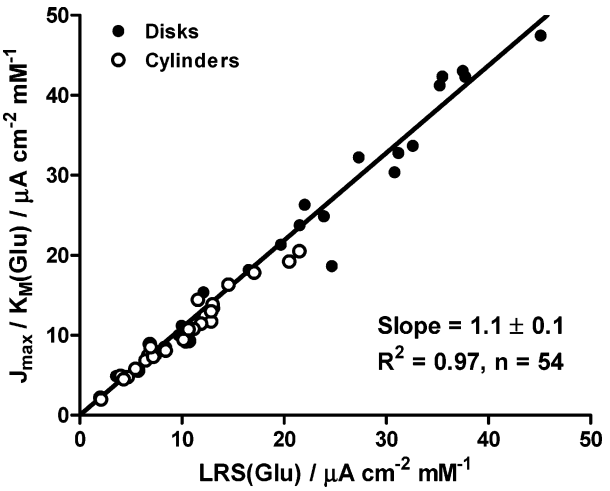

Figure 2. A linear regression test of eq 8 for the Pt/GluOx/PPD configuration of both geometries was executed by determining the two Michaelis−Menten parameters for each biosensor (Figure 1), calculating their ratio as J_{max}/K_M, and plotting this ratio against the experimentally measured Glu LRS for the corresponding electrode. Equation 8 predicts a slope of unity. There was no significant difference between the regression slope for Pt_C/GluOx/PPD (0.95 ± 0.04, R^2 = 0.96, n = 30) and that for Pt_D/GluOx/PPD (1.10 ± 0.05, R^2 = 0.96, n = 24); these two populations were therefore pooled (1.1 ± 0.1, R^2 = 0.97, n = 54).

However, although eq 9 was equally valid for Pt_C/GluOx/PPD and Pt_D/GluOx/PPD configurations (Figure 2), the difference between the average values of the LRS for the two designs reported recently[40] was confirmed for these larger populations of electrodes (nA cm^{-2} μM^{-1}): LRS_C = 13 ± 2 (n = 34); LRS_D = 28 ± 2 (n = 46; p < 0.0001) (see Table 1). Both the geometric area and LRS of these Pt_D-based biosensors were similar to the more complicated carbon fiber cylinder designs involving catalytic oxidation of H_2O_2 using redox polymers and horseradish peroxidase.[15] The values of J_{max} and K_M(Glu) for the cylinder- and disk-based biosensors were examined in an attempt to understand this difference.

***J*$_{max}$ and K_M(Glu) for the Pt/GluOx/PPD Design.** The most distinctive feature of Figure 1 is the significantly larger J_{max} value for disks versus cylinders. Classical electrochemistry would suggest that the diffusion of analyte to an electrode surface should be more efficient via hemispherical[77] versus cylindrical[78] diffusion. However, the finding that the response of electroactive species, such as ascorbate at bare Pt[62] and H_2O_2 at PPD-coated Pt,[41] differ little for electrodes of the size and geometry used here over similar (long) time scales indicates that diffusion of Glu to the biosensor cannot account for the differences between Pt_C/biosensors and Pt_D/biosensors illustrated in Figure 1.

Large populations of Pt_C and Pt_D biosensors of this GluOx/PPD design were calibrated in the same way to investigate the reproducibility of differences shown in Figure 1 (see Table 1). On average, the J_{max} value, and therefore enzyme loading,[41] for Pt_D/GluOx/PPD was 15 times greater than for Pt_C/GluOx/PPD. This is consistent with retention of a dome of enzyme solution around the disk tip as it is removed vertically from the GluOx

(71) Castillo, J.; Davalos, A.; Lema, M.; Serena, J.; Noya, M. *Cerebrovasc. Dis.* **1997**, *7*, 245−250.
(72) Ince, E.; Karagoel, U.; Deda, G. *Acta Paediatr.* **1997**, *86*, 1333−1336.
(73) Segovia, G.; Porras, A.; Mora, F. *Neurochem. Res.* **1997**, *22*, 1491−1497.
(74) Lada, M. W.; Kennedy, R. T. *Anal. Chem.* **1996**, *68*, 2790−2797.
(75) Miele, M.; Berners, M.; Boutelle, M. G.; Kusakabe, H.; Fillenz, M. *Brain Res.* **1996**, *707*, 131−133.
(76) Davalos, A.; Shuaib, A.; Wahlgren, N. G. *J. Stroke Cerebrovasc. Dis.* **2000**, *9*, 2−8.
(77) Dayton, M. A.; Brown, J. C.; Stutts, K. J.; Wightman, R. M. *Anal. Chem.* **1980**, *52*, 946−950.
(78) Jacobsen, T.; West, K. *Electrochim. Acta* **1995**, *40*, 255−262.

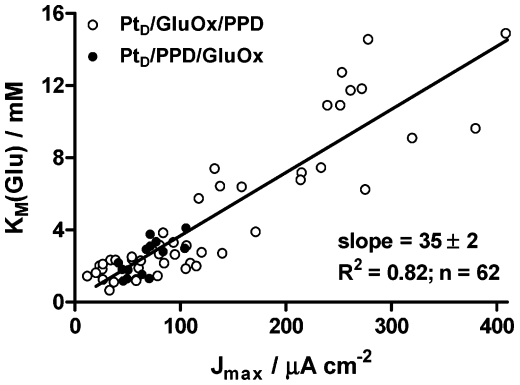

Figure 3. Scatter plot and linear correlation analysis for K_M(Glu) vs J_{max} values, obtained using eq 4 (see Figure 1), for Pt$_D$/GluOx/PPD (slope = 35 ± 3 μM μA^{-1} cm^2, R^2 = 0.81, n = 46) and Pt$_D$/PPD/GluOx (slope = 34 ± 9 μM μA^{-1} cm^2, R^2 = 0.51, n = 16) biosensors. There was no significant difference between these slopes; the two populations were therefore pooled (35 ± 2 μM μA^{-1} cm^2, R^2 = 0.82, n = 62).

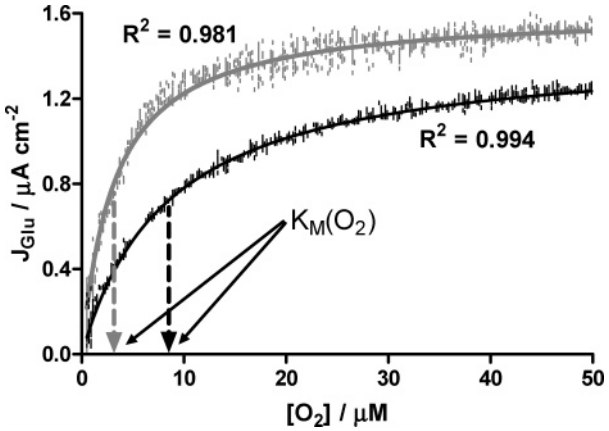

Figure 4. Examples of unfiltered data, recorded amperometrically (+700 mV vs SCE) at 10 Hz with two Pt$_D$/GluOx/PPD biosensors of the same size and design, but showing different Glu sensitivity (LRS values) and plotted against oxygen concentration recorded simultaneously using a CellOx sensor. The curve in each case represents the nonlinear regression analysis using eq 7. Surprisingly, even for biosensors of the same geometry, size, and design, the device with the higher Glu LRS showed a lower oxygen dependence, $K_M(O_2)$. The regression parameters obtained for these examples (50 μM Glu) were J'_{max} = 1.62 ± 0.01 μA cm^{-2}, $K_M(O_2)$ = 3.20 ± 0.04 μM, R^2 = 0.981 (higher LRS sensor); and J'_{max} = 1.45 ± 0.01 μA cm^{-2}, $K_M(O_2)$ = 8.53 ± 0.07 μM, R^2 = 0.994 (lower LRS sensor).

solution during the dip−evaporation procedure, as expected from surface tension considerations. Upon evaporation, the density of GluOx on the disk surface was, therefore, higher than that achieved when the corresponding cylinder geometry was prepared. A similar effect has been observed in the preparation of GOx-based glucose biosensors.[41]

More surprising, however, was the 7-fold increase in the mean K_M(Glu) value for these disk biosensors (Pt$_D$/GluOx/PPD) as compared with the cylinders (Pt$_C$/GluOx/PPD; see Table 1). Thus, the design with the higher mean J_{max} displayed the higher K_M(Glu) value and explained why the 15-fold increase in J_{max} achieved for the disks led to only a 2-fold increase in the LRS (see eq 9). To determine whether this disparity in K_M(Glu) was due to size/shape differences between the two designs, a correlation analysis for K_M(Glu) versus J_{max} was performed on the design with the greater range of J_{max} values, Pt$_D$/GluOx/PPD. There was a strong (slope = 35 ± 3 μM μA^{-1} cm^2, n = 46) and significant correlation (R^2 = 0.81, p < 0.0001) between these two variables (see Figure 3). The Pt$_D$/GluOx/PPD sensors that were fabricated with the greater number of GluOx dips generally showed the higher J_{max} value in subsequent Glu calibrations, although there was a degree of variation within each dip group. The important finding here was that the K_M(Glu) value increased significantly with increasing J_{max} and explains why K_M(Glu) was lower on cylinders, namely, the small J_{max} value for cylinders (Table 1). Thus, Pt$_C$/GluOx/PPD electrodes behaved essentially like Pt$_D$/GluOx/PPD sensors with low enzyme loading.

***J*$_{max}$ and *K*$_M$(Glu) for the Pt/PPD/GluOx Design.** The recent finding that depositing GOx over the PPD polymer in the fabrication of glucose biosensors led to a substantial increase in the analyte LRS[41] prompted us to explore the corresponding configuration involving GluOx: Pt$_C$/PPD/GluOx and Pt$_D$/PPD/GluOx. In contrast to the behavior of GOx-based biosensors, depositing the GluOx after the electropolymerization step led to no significant change in the mean LRS for Glu (Table 1). To investigate this further, a correlation analysis for K_M(Glu) versus J_{max} was performed on the Pt$_D$/PPD/GluOx design and compared with the Pt$_D$/GluOx/PPD directly (see Figure 3). There was no distinguishing difference between the regression parameters of these two disk designs, except that the sample of 16 Pt$_D$/PPD/GluOx electrodes tended to clump at the lower end of the distribution with the majority of the alternative design. Thus, the mean of both J_{max} and K_M(Glu) for Pt$_D$/GluOx/PPD was approximately one-half that of Pt$_D$/PPD/GluOx (Table 1).

This analysis and a comparison with its equivalent for PPD-GOx biosensors[41] reveals an important difference between the behavior of GOx and GluOx immobilized on solid surfaces. K_M(G) for GOx-based sensors was very sensitive to the PEC layer configuration (GOx/PPD versus PPD/GOx); for example, being significantly lower for Pt$_D$/PPD/GOx than for Pt$_D$/GOx/PPD.[41] It appeared that GOx loading itself did not greatly influence K_M(G), but the PPD polymer did so, representing a steric barrier to the neutral glucose molecule (equivalent reaction 1 for glucose, and eq 6). In contrast, the major determinant of the value of K_M(Glu) was GluOx loading, with the order of PPD deposition playing a relatively less significant part (Figure 3). These data are consistent with the hypothesis that for anionic substrates such as Glu interacting with polyanionic proteins (pI for GluOx is 6.2),[19] high loading of enzyme leads to an electrostatic barrier, reducing the affinity of enzyme for its substrate.[79] The overall outcome of this interaction is that increasing the density of GluOx on the disk surface increases the K_M(Glu) significantly (see Figure 3) but has little effect on the LRS; indeed, there was no correlation (R^2 = 0.01, n = 62) between Glu sensitivity in the linear response region (LRS) and enzyme loading (J_{max}) over the range of J_{max} shown in Figure 3.

Oxygen Sensitivity Studies. Figure 4 shows the effect of changing the concentration of oxygen in the electrochemical cell, from submicromolar levels to 50 μM, on the biosensor signal recorded for 50 μM Glu using two Pt$_D$/GluOx/PPD electrodes

(79) McMahon, C. P.; Rocchitta, G.; Serra, P. A.; Kirwan, S. M.; Lowry, J. P.; O'Neill, R. D. *Analyst* **2006**, *131*, 68−72.

that displayed different Glu LRS sensitivity. The oxygen dependence can be quantified as $K_M(O_2)$, defined in eq 7.[40,41,47] Unexpectedly, the biosensor with the greater Glu sensitivity (LRS) showed the smaller $K_M(O_2)$ value, that is, displayed a lower oxygen dependence. This anomaly is in line with that described for differences in the oxygen dependence of cylinder and disk Glu biosensors[40] but is more remarkable because the comparison shown in Figure 4 is between data recorded with two biosensors of the same design, Pt_D/GluOx/PPD.

We established recently that $K_M(O_2)$ increases linearly with Glu concentration in the experimental range 5−150 μM Glu, with a limit of 0 μM oxygen as the concentration of Glu approaches 0.[40] The slope of these $K_M(O_2)$ versus Glu concentration plots defines the oxygen dependence of the sensor design in terms of micromolar oxygen per micromolar Glu ($\mu M(O_2)\ \mu M(Glu)^{-1}$). The $K_M(O_2)$ values were, therefore, determined over a range of Glu concentrations for each of the four biosensor designs. There was no significant difference between the corresponding linear regression slopes for the GluOx/PPD and PPD/GluOx configurations within the two populations defined by geometry, and so the slopes were pooled: Pt_C/GluOx∼PPD ($0.24 \pm 0.02\ \mu M(O_2)\ \mu M(Glu)^{-1}$, $n = 8$); and Pt_D/GluOx∼PPD ($0.07 \pm 0.01\ \mu M(O_2)\ \mu M(Glu)^{-1}$, $n = 17$); $p < 0.001$ for cylinder versus disk designs.

To investigate this difference in $K_M(O_2)$ between disks and cylinders and between disk-based biosensors of the same design (Figure 4), correlation analyses were performed for $K_M(O_2)$ versus the Glu Michaelis−Menten parameters: J_{max} for GluOx loading (eq 4) and K_M(Glu) as a measure of enzyme affinity for substrate (see eqs 5 and 6). Reciprocals of the Michaelis−Menten parameters were used for the following reasons. A common strategy of increasing biosensor sensitivity is to increase the loading of active enzyme; it is particularly important, therefore, to understand the influence of high GluOx surface density on biosensor oxygen sensitivity. As enzyme loading increases, $1/J_{max}$ approaches 0, and it is more reliable to focus in on this region of the plot, as opposed to an indefinitely increasing value of J_{max}.

The continuity of the behavior of cylinder versus disk biosensors in Figure 2 and PPD/GluOx versus GluOx/PPD polymer/enzyme configurations in Figure 3 suggests that the major determinant of biosensor behavior is enzyme loading. As GluOx loading increased, K_M(Glu) increased proportionately (Figure 3), but it is not immediately obvious which of the three rate constants in eq 6 are involved in this change. For a system in which the main determinant is enzyme loading, we argue that once the enzyme/substrate complex is formed (eq 5), GluOx surface density will have little effect on k_{-1} and k_2. More specifically, we suggest that the increase in K_M(Glu) observed with increased J_{max} is due mainly to a decrease in k_1 associated with unfavorable interactions between anionic Glu and the high density of surface protein. Therefore, to investigate the relationship between $K_M(O_2)$ and K_M(Glu), $1/K_M$(Glu) was used as a direct function of k_1.

Figure 5 (bottom) shows a single linear correlation ($R^2 = 0.77$, $n = 25$) between $K_M(O_2)$ and $1/K_M$(Glu) for the combined populations of cylinder and disk biosensors. The intercept on the $K_M(O_2)$ axis was effectively 0 (0.02 ± 0.02, $n = 25$), indicating that the oxygen dependence vanished as k_1 (eq 6) approached 0, as expected (no H_2O_2 produced in reaction 2). $K_M(O_2)$ increased steadily as k_1 increased over the entire range of J_{max} observed in this study (up to 400 $\mu A\ cm^{-2}$). This again is expected as a result of an increase in the rate of H_2O_2 generation. Thus, Figure 5 (bottom) is totally in line with expectation on the basis of reactions 1 and 2.

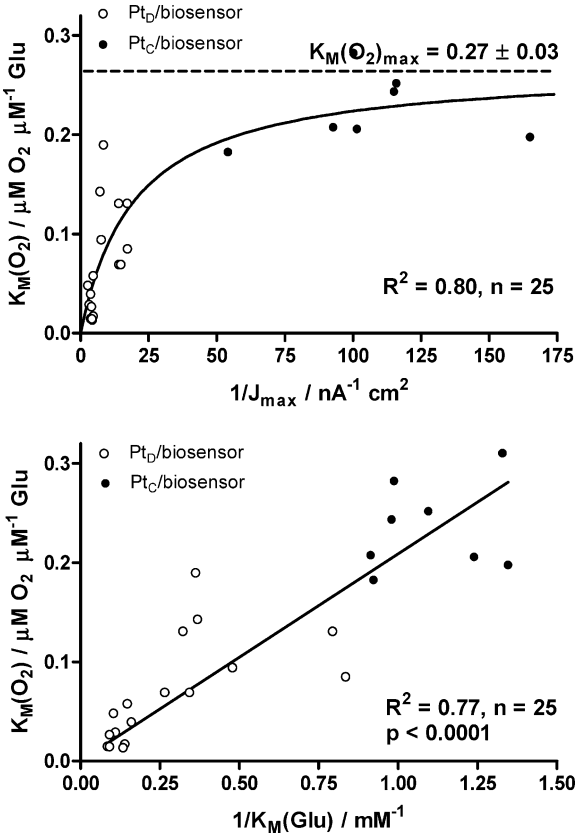

Figure 5. Scatter plots and regression analyses for biosensor oxygen dependence, $K_M(O_2)$, versus reciprocal of active enzyme loading, $1/J_{max}$ (top), and $1/K_M$(Glu) (bottom), used as a measure of enzyme affinity for substrate, k_1 in eq 5 (see eq 6). As in Figure 3, there was no difference in the behavior of PPD/GluOx versus GluOx/PPD polymer/enzyme configurations, and therefore, single populations were formed for each of the geometrical designs, Pt_C/biosensor and Pt_D/biosensor. Although dispersed at either end of the distributions, the cylinder and disk forms of the biosensor displayed a continuity of behavior, suggesting enzyme loading is the main difference between these designs.

The overall relationship between the data points for the $K_M(O_2)$ versus $1/J_{max}$ plot (Figure 5, top) is not as clear-cut. There is a greater clustering of the disk and cylinder points, due to the large difference between the mean J_{max} values for the two geometries (Table 1). To help choose a suitable fit for these data, we reiterate the continuity in behavior shown by the different designs in a variety of analyses (Figures 2, 3, and 5 (bottom)). In addition, although the data in Figure 5 (top) do not represent clear evidence for this "continuum" hypothesis, they are not inconsistent with it. Therefore, a reasonable approach was to choose the simplest relationship that fitted all the $K_M(O_2)$ versus $1/J_{max}$ data adequately, a hyperbola ($R^2 = 0.80$, $n = 25$).

For very low GluOx loading, the oxygen dependence approached an asymptotic value of $0.27 \pm 0.03\ \mu M(O_2)\ \mu M(Glu)^{-1}$, corresponding to the limit of infinite dispersion of enzyme molecules on the electrode surface (Figure 5, top). This limiting behavior of $K_M(O_2)$ is not unexpected. The apparent anomaly in these data is the direction of change away from the asymptote

for higher GluOx loadings: decreasing rather that increasing. Thus, as the enzyme loading increased, the oxygen dependence decreased toward 0 (data points and curve), a totally counterintuitive, and potentially valuable, finding in the context of Glu biosensor design. This behavior of the GluOx system stems from the relationship illustrated in Figure 3 (steady, major increase in K_M(Glu) with J_{max}) and the consequence of this for the oxygen dependence of these biosensors. As GluOx loading was increased, K_M(Glu) increased, probably due to a reduction in k_1, but this had the effect of reducing oxygen demand on a molecular (enzyme) level (Figure 5, bottom). This explains the anomaly displayed by the average $K_M(O_2)$ values above, as well as preliminary results reported recently.[40] Therefore, increased GluOx loading had dual beneficial effects of a modest increase in Glu sensitivity in the LRS (Table 1) and a reduction in oxygen dependency in the LRS range of Glu concentrations (Figure 5, top).

These PPD-based sensors compare favorably with an optimized redox polymer design reported recently, but whose oxygen dependence has yet to be determined.[80] The redox polymer-modified carbon fiber design, which has a geometric surface area similar to Pt_D electrodes, showed about a 3-fold higher sensitivity than the PPD-modified disk designs described here; this advantage was achieved, at least in part, by the thicker hydrogel matrix involved. The consequent disadvantage of thick layers, however, was a response time that was an order of magnitude slower than the PPD designs, a significant limitation for monitoring potentially fast Glu transients in vivo. We are currently investigating the characteristics of the PPD-based Glu biosensors in behaving animals in terms of their sensitivity, selectivity, and stability.

CONCLUSIONS

The data and analysis presented here provide an explanation for the apparent anomalous behavior of Glu biosensors based on Pt disks and cylinders presented recently[40] and show that enzyme loading, not geometry, was the underlying difference between the Glu and oxygen responses of these two designs. This study also shows that the alternative arrangement of depositing enzyme after electropolymerization of the PPD had no significant effect on biosensor parameters, a marked divergence from the properties of glucose biosensors incorporating GOx.[41] Control of the oxygen dependence of these devices was possible by varying the loading of GluOx, a behavior that was rationalized in terms of the relationships between J_{max}, K_M(Glu), and $K_M(O_2)$. Of the four designs, the Pt_D/GluOx/PPD electrode offered the highest LRS current density and lowest oxygen dependence. However, even the cylinder designs that showed the lowest enzyme loading and, therefore, the highest $K_M(O_2)$ were capable of working at 90% efficiency down to concentrations of oxygen as low as 20 μM for 10 μM Glu.[40]

The suitability of the design for a given application depends on the concentration of Glu being monitored, as well as the range of fluctuations in pO_2 relevant to that medium. For example, Glu concentrations under physiological conditions are normally below 10 μM for cerebrospinal fluid[71,72] and brain ECF,[73−75] but 100 μM levels have been detected in the ECF following brain trauma.[76] Thus, if the trauma also involved anoxia, then the combination of excessive Glu and low pO_2 could undermine the functionality of the Glu biosensor. We are presently exploring the behavior of these biosensors in the intact brain in terms of sensitivity, selectivity, and stability in vivo. The oxygen dependence of PEC-based biosensors, whose Glu sensitivity has been increased significantly by the incorporation of polyelectrolytes,[79] is also under investigation.

ACKNOWLEDGMENT

This work was funded in part by Science Foundation Ireland (03/IN3/B376 and 04/BR/C0198). We thank Dr. Kusakabe of Yamasa Corp., Japan for a generous gift of glutamate oxidase, and Enterprise Ireland for a postgraduate scholarship (C.McM).

Received for review October 11, 2005. Accepted February 1, 2006.

AC0518194

(80) Oldenziel, W. H.; Westerink, B. H. C. *Anal. Chem.* **2005**, *77*, 5520−5528.